System optimization of SiC inverters regarding efficiency, cost and reliability

Dr. Thomas Orlik, Dr. Michael Maiworm, Dr. Mathias Lindner, Dr. Christoph Danzer, Heiko Rabba, and Matthias Schultalbers

IAV GmbH, Carnotstraße 1, 10587 Berlin

Abstract. Current challenges in the development of new electric traction drives are focusing on increasing efficiency and power while minimizing installation space and system costs. On one hand the use of new SiC power modules has led to an increase of efficiency. On the other hand, higher component costs must be amortized by an increased utilization of the inverter which is challenging for the lifetime and reliability of the inverter. The increasing spread of electric powertrains in commercial vehicles and rising safety requirements due to future automated driving functions place increasing demands on the reliability of the drive system which have to be considered during component design. Potential for a system optimization of SiC traction inverters and a reconciliation of efficiency, costs and reliability arise from optimized control strategies and a connection of IAV's technology-oriented powertrain synthesis method with thermal and lifetime simulations of the inverter.
Keywords: System design, SiC inverter, reliability, lifetime.

1 Introduction

Current challenges in the development of new electric traction drives are focusing on increasing efficiency and power, while minimizing installation space and system costs. For the traction inverter the transition from IGBT technology to Silicon Carbide (SiC) MOSFETs has led to a significant reduction of power losses and thus to an increased system efficiency. Even though silicon carbide MOSFETs were initially mainly represented in the premium segment and 800V electrical systems, they are now also emerging in other vehicle segments and 400V electrical systems.

	650V SiC MOSFET	**1200V SiC MOSFET**
Die area	5x smaller	5x smaller
Power density	2x greater	16x greater
Switching losses	6.5x lower	11x lower
Fall time	1.5x faster	7x faster
Price	3x higher	3.5x higher

Table 1. Comparison of SiC MOSFET characteristics with equivalent IGBTs [2]

A comparison of the characteristics of 650V-SiC-MOSFET shows that the technology clearly outperforms IGBT technology also in the medium voltage range, although the advantage is smaller when compared to 1200V devices [2]. The main drawback of silicon carbide devices is the approximately three times higher price compared to IGBTs [1]. This leads to higher costs of the whole e-drive system and must be amortized through the increased system efficiency, e.g., a reduced battery size at a constant driving range due to lower power losses.
In addition, higher costs require a high utilization of the inverter and a reduction of safety margins in the component design. This leads to an operation at high temperatures and is challenging for the lifetime and reliability of the inverter.
On the other hand, the increasing spread of electric powertrains in commercial vehicles and rising safety requirements due to future automated driving functions place increasing demands on the reliability of the drive system.
The main task is to optimally reconcile these particularly high demands placed on power electronics for traction drives during the concept phase: high efficiency, minimal costs, and compactness at increasing system reliability. To address this, IAV connected it´s technology-oriented powertrain synthesis methods with thermal and lifetime simulations of the inverter in one method-chain.

2 Synthesis of optimized electric drive systems

Optimizing the components of the electric powertrain, topologies and functions requires a development process on the system level for powertrain and vehicle, as well as a long-term product strategy for the whole vehicle fleet. IAV offers unique methods and tools for proceeding systematically the whole development process, from the end user requirement through to the system release recommendation.
The systematic process (**Fig. 1**) starts by recording all the requirements made by the end user, legislation, the target markets, the vehicle manufacturer, suppliers, and energy providers. IAV then uses mobility synthesis to describe the influence of market and environmental conditions on the user behavior, thus developing future mobility scenarios that can be described in terms of their technical requirements and customer acceptance. Based on these mobility scenarios, IAV systematically ascertains and optimizes powertrain concepts that are expedient solutions for the specific vehicle and primary energy source to achieve carbon-neutral mobility.

Powertrain synthesis systematically varies the large number of all possible power-train components and its technologies, such as all relevant e-machine types, and battery technologies and inverter topologies.
Afterwards the resulting powertrain variants are optimized in terms of cost, efficiency and driving performance. The main component parameters are thus defined as the basis for then developing the detailed designs of the respective components, using the proven synthesis methods among others for transmission, electric motor, and inverter.

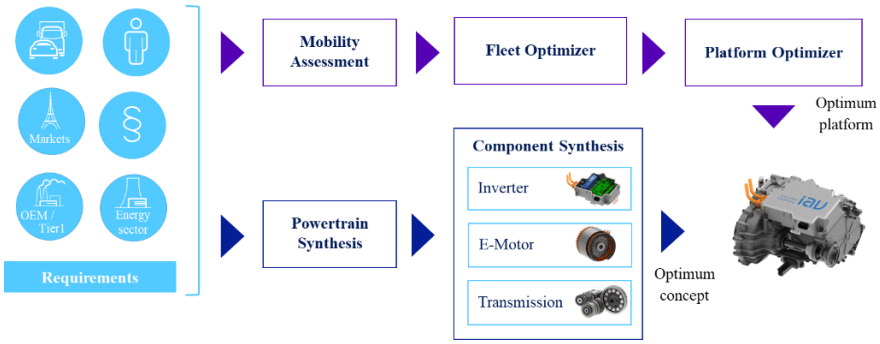

Fig. 1. IAV Methods for advanced development

The inverter design is embedded into the powertrain synthesis workflow and provides all necessary data for a concept evaluation with respect to efficiency, cost, and volume. The automated design process determines the specification for the power module and the DC link capacitor, which have a major influence on cost and volume of the inverter.

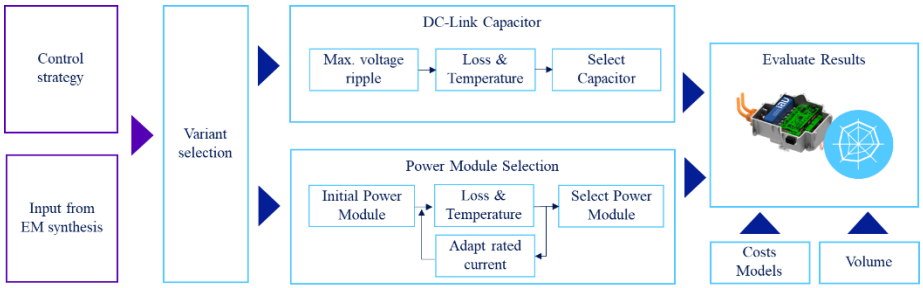

Fig. 2. Inverter concept evaluation during powertrain synthesis

The inputs for the inverter design such as maximum AC currents, DC voltage and power factor are provided by the EM synthesis for each powertrain variant. Several inverter designs are evaluated afterwards, depending on the selected parameters number of phases, topology, and semiconductor technology. For the optimization, the control strategy defines the optimal PWM strategy.

The DC link capacitor is designed to ensure a maximum DC voltage ripple according to ISO 21498-2 or other relevant OEM standards. Based on different parameter sets the power loss and estimated temperature are calculated and a capacitor is selected.

The rating of the power module is determined for the worst-case thermal conditions at zero or very low speed and maximum current. Scalable loss models and a steady state thermal model of the power module are used to obtain the rated current and a selection of a matching of the power module. The results are evaluated with respect to costs, volume, and efficiency.

During powertrain synthesis, this initial design of the inverter is carried out for every possible variant that fulfills the general powertrain requirements. The result consists in a powertrain concept with specific individual components that are evaluated against

specific KPIs: powertrain costs, driving performance, electric range, and sustainability (**Fig. 3**).

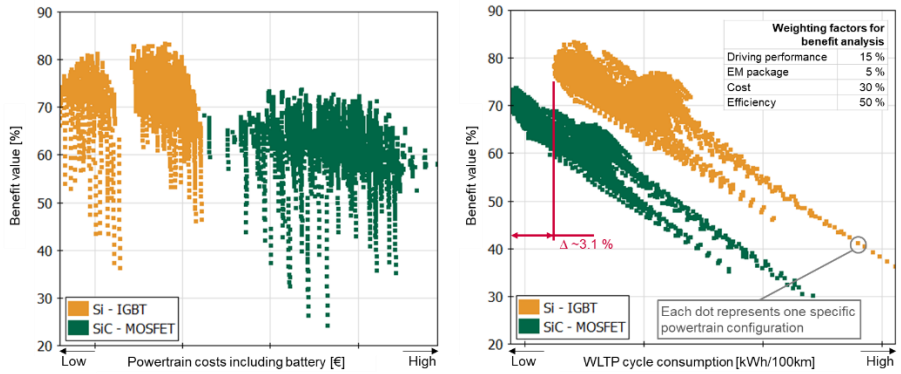

Fig. 3. Exemplary comparison of different semiconductor technologies and its impact on the powertrain costs and energy consumption for IAV dedicated e-drive platform

At the same time, the vehicle-specific powertrain variants form the basis for optimization on fleet level. Platform synthesis collates the vehicle-specific optimized powertrain variants in modular systems for systematic minimization of diversity, emissions, and costs on fleet level (**Fig. 1**). This extensive approach thus permits a dedicated and sustainable development of future mobility.

3 Optimized operating strategies for traction inverters

The operating strategy for the control of the electric drive and the inverter is of great importance. The control strategy determines not only the efficiency, but also the thermal load of the components and must ensure operation even in the thermal limit range. The goal should therefore be a control strategy that maximizes efficiency on the one hand and minimizes the impact on component lifetime on the other. Thus, it is crucial to consider the control strategy of the inverter and its interactions on other components such as the e-machine or the HV-system already in the design phase.

3.1 Reliability of SiC power modules

The lifetime of power semiconductors is influenced by different external factors. Ageing due to thermal stress and high temperatures is one of the main failure mechanisms of SiC MOSFETs as well as IGBT power modules.
These effects can be grouped as package-based failure mechanisms since they cause a degradation of the packaging technology (**Fig. 4**). Other failure mechanisms such as semiconductor degradation must be considered during the design of the power module but play a minor role during operation of the inverter.

The power module itself consists of different layers of materials (**Fig. 5**). In the case of package-based mechanisms, temperature swings result in various effects caused by a temperature-related expansion of the materials. A wear of the solder layer increasing with the number of working cycles provides a worse thermal conductivity. In addition, strong temperature fluctuations have a negative effect on the bond wires. Analogous to the solder layers, the bond wires wear out with increasing working time, which leads to a degradation of the metal [3]. In the worst case, this will cause the bond wires to lift off or break, resulting in a destruction of the power module.

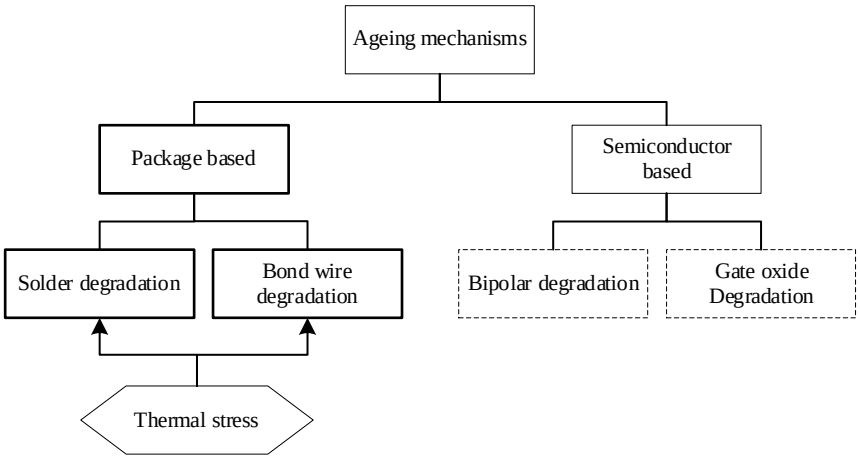

Fig. 4. Ageing mechanisms of power modules

Compared to silicon based power modules, different material properties of silicon carbide lead to an approximately 40% higher plastic strain [4], which makes SiC MOSFETs more sensitive towards temperature changes [5].
Advances in the power module packaging has led to an improvement of the reliability of SiC power devices at higher junction temperatures, increasing switching frequencies, and smaller chip areas [6].

During inverter development, the reliability of the power module is predicted by mission profile-based simulations (**Fig. 6**). The mission profiles are based on vehicle load cycles. Despite various driving cycles, passive thermal loading such as charging or preconditioning are also included. The corresponding loading for the inverter, such as AC current, AC voltage, or power factor are provided by the e-machine synthesis. The inverter losses and temperatures are calculated with respect to the inverter topology, control strategy (PWM method, switching frequency, etc.), and a temperature model of the power module. After a Rainflow counting of the temperature cycles, a lifetime estimate is obtained by lifetime models such as CIPS 08 or LESIT [11].

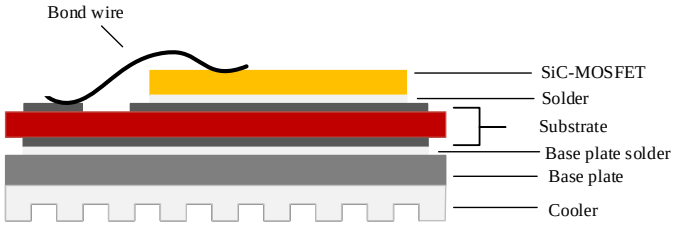

Fig. 5. Simplified cross section of a SiC power module

The CIPS08 and LESIT models are well-established for the lifetime modelling of IGBT and have been developed by experiments on silicon devices. Recent investigations show that the original model parameters cannot be directly transferred to SiC MOSFETs [5] but need to be parametrized for the specific power module by measurements. For automotive power modules, the power cycling tests according to AQG-324 are used to evaluate the thermo-mechanical lifetime and the parameters of the lifetime model. In the following, a LESIT model is used for the lifetime predictions.
It becomes clear that the reliability of SiC MOSFETs depends to a large extent on the operating temperature. An improvement can be achieved by reducing or controlling the temperatures of the MOSFET during operation.

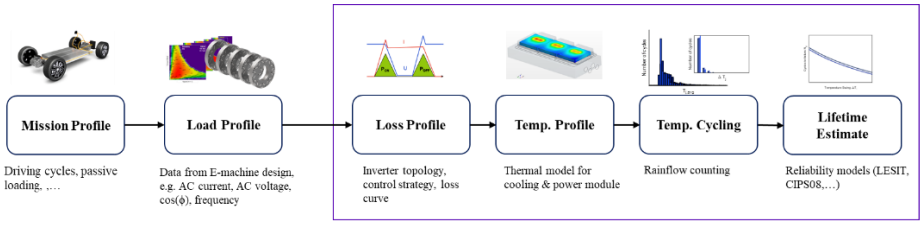

Fig. 6. Simulation workflow for mission profile-based lifetime estimation

3.2 Active thermal management of traction inverters

As shown in the previous section, the temperature is a main influencing factor on the power module's lifetime. Hence, an optimal control strategy should be used to minimize the thermal stress of the power device. This is typically achieved using active thermal control, which tries to decrease the thermal stress on the involved power electronic devices by decreasing the maximum temperature, as well as the temperature change [10]. Typical approaches manipulate the inverter cooling, the peak load current, or the modulation scheme. Another frequent approach is to adjust the switching frequency. In particular, the switching frequency is dynamically reduced to decrease the

instantaneous power (switching) losses and with that the resulting temperatures [7, 8, 9]. In [13] a method for a chip size optimization of the power module based on active thermal control is discussed. It allows a smaller sizing of the power module and thus a cost reduction of the inverter.

3.3 Implications for the powertrain

The switching frequency influences the thermal stress and with that the lifetime of the power electronics. However, it has also effects on other subsystems and aspects of the powertrain. For instance, it influences the resulting DC link voltage ripple, as well as the efficiency (losses) and the control performance of the e-machine. A manipulation strategy of the switching frequency that is advantageous for the inverter lifetime can have negative effects on these other subsystems. For this reason, we consider not only the inverter but combine it with the aforementioned subsystems in one powertrain simulation/synthesis. Thus, the objectives of the remainder of this work are:

1. Consider the combined power losses of inverter and e-machine.
2. Vary the switching frequency to minimize the combined power losses.
3. Satisfy DC link voltage ripple constraints.
4. Increase the inverter lifetime.

4 Powertrain Simulations

4.1 Inverter Simulation

The involved inverter simulations comprise the following two parts:

1. A dedicated simulation for the DC link voltage ripple.
2. A combined power loss and thermal model that outputs predicted average values w.r.t. the phase current's fundamental period.

Calculation of the minimal switching frequency

The active thermal control typically reduces the switching frequency to reduce the thermal stress on the power electronics. However, it cannot be made arbitrarily small because certain constraints must be satisfied. On one hand, the DC link voltage ripple must be below certain maximum values for different operating points (the smaller the switching frequency, the larger the ripple). These are specified in the ISO 21498-2 norm or the corresponding OEM standards respectively. On the other hand, the switching frequency must be large enough to ensure the sinusoidal shape of the output current.

To satisfy the maximum DC link voltage ripple, we set up a simulation model that includes the DC link subsystem to compute the voltage ripple. The ripple is a function of phase current I, power factor $\cos(\varphi)$, modulation level M and switching frequency f_{sw}. All these inputs are varied and for each combination of $(I, \cos(\varphi), M)$ the minimal switching frequency $f_{\mathrm{sw,min}}$ that still satisfies the maximum voltage ripple is determined. The results are then stored in a lookup table $f_{\mathrm{sw,min}} = LUT(I, \cos(\varphi), M)$.

To ensure the sinusoidal shape of the output current, we enforce

$$10 f_{\mathrm{Sttr}} \leq f_{\mathrm{sw,min}}$$

with the stator frequency f_{Sttr}.
In the following simulations we pick the larger of the two calculated $f_{\mathrm{sw,min}}$ values to satisfy both constraints. An absolute minimum switching frequency of 1 kHz is chosen for the optimization.

Average Inverter Model

The inverter model consists of two parts. The first part computes the power losses of the SiC MOSFET and its body diode. The second part computes the (common) junction temperature. All involved quantities are calculated as average values for the fundamental period $T_{\mathrm{Sttr}} = 1/f_{\mathrm{Sttr}}$ of the stator current.

The calculation needs to be executed only once at the beginning of each period, which is advantageous because it does not need to be executed with the switching frequency and saves computational resources. This is particularly important for the integration in the powertrain synthesis, as this computes all variants and all possible states of the overall system. Another advantage with the specific employed average model [7] (more details below) is that it not only allows a prediction for the junction temperature but for the maximum temperature and its change within the stator period too.

The average power loss model is based on [11] (SVPWM modulation) and extended also to the DPWM1 modulation scheme for large modulation factors. Furthermore, as the MOSFET (other than an IGBT) can conduct currents in forward and backward direction, the model is adapted accordingly.

The temperature model is based on a Foster model (parameters can be taken from the data sheet), whose input is the average power loss P_{avg} for one MOSFET-diode pair. Since a SiC MOSFET has a common junction with its body diode, P_{avg} heats up MOSFET and diode equally. Being an average model, the Foster model can be simplified to the static thermal resistance R_{th}. However, the dynamic Foster model, as provided in the data sheet, is used offline to generate lookup tables $T_{j,max} = LUT(f_{\mathrm{Sttr}}, P_{\mathrm{avg}})$ for the maximum temperature and $\Delta T_j = LUT(f_{\mathrm{Sttr}}, P_{\mathrm{avg}})$ for the temperature change. They can then be evaluated online and yield a prediction during the fundamental stator period.

The average model's accuracy is verified using a model that computes power losses and temperatures for the switching period [11]. Afterwards it is integrated in the synthesis simulation of the powertrain, which enables to compute optimal sequences of a changing switching frequency w.r.t. the overall losses of the system.

4.2 E-machine simulations

The considered e-machine is a permanent-magnet excited synchronous machine (PSM) with double V-shaped magnets in 8 poles and a distributed round-wire winding. As such, it depicts a typical automotive traction motor for a D- or E-segment with optimized efficiency behavior and designed for a battery voltage of 370V.

An FEA model using JMAG has been created considering all relevant losses, as copper loss, hysteresis/eddy current/excess loss, and magnet loss. The excitation has been realized with PWM switched voltages from a constant DC voltage according to third-harmonic injection modulation. Windage and friction loss are estimated analytically. This model has been solved for a cross-combination of several rotor speeds, d- and q-axis currents, as well as four PWM switching frequencies: 1, 4, 7, and 10 kHz.

In a post-process, quasi-static operational points regarding torque/speed have been deduced with the MTPA/MTPV method. This resulted in a set of e-machine loss maps for each simulated constant switching frequency. Furthermore, also inverter loss maps and maps of the junction temperatures were calculated at this step because the required inputs (phase current, power factor, and modulation degree) were then known for each operational point.

4.3 Cycle simulations

Determination of the loss optimal switching frequency

For each operational point, resp. torque/speed combination, as well as PWM switching frequency, the system loss as a sum of e-machine and inverter loss are known from the previous e-machine simulations. These system losses have been interpolated over the switching frequency. Afterwards, an optimizer was used to find switching frequencies that generate minimal system losses in each operational point. The lower boundaries for the optimizer runs were found in the minimal frequencies from Sec. 4.1.

As a result, a map of operational points with their individual loss-optimal switching frequencies has been developed. This is shown in **Fig. 7** and shows an interesting effect: in areas approaching the peak performance the frequency is rather low and changes rapidly between similar operational points. Here, the optimal frequencies correspond to the minimal switching frequencies because the correlation of switching frequency to inverter loss is much stronger than to e-machine loss. In other words, reducing the switching frequency saves more inverter loss than it costs e-machine loss.

By contrast, in areas with either low torque or low speed the frequency tends to be reasonably high and stable. Here the correlation to e-machine loss dominates because on one hand the inverter loss is low due to low phase current or voltage. On the other hand, the e-machine losses are dominated by iron loss, which are highly influenced by the switching frequency. The bigger areas of numerically constant frequencies are rather a result of the discretization in FEA calculations. With four frequency sampling points used in FEA the optimizer on an interpolation of those four points always yields one of them. A smooth gradient of optimal frequency would be expected instead.

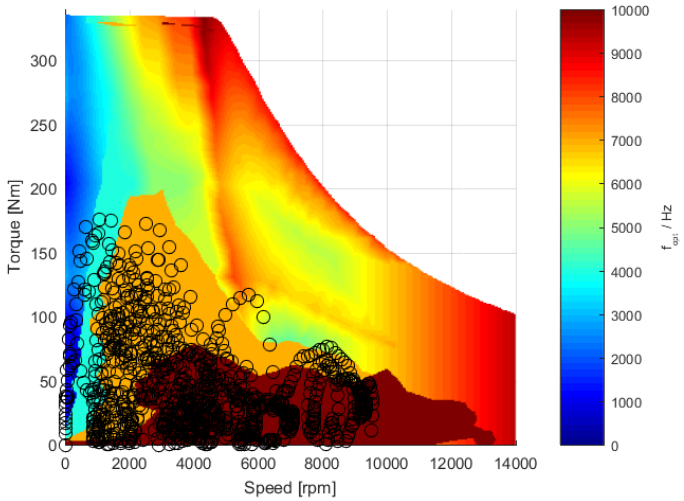

Fig. 7. Loss-optimal switching frequencies with WLTC operational points

Calculation of WLTC cycle behavior

The operational points for WLTC cycle simulation have been deduced from a D-segment passenger car with the IAV powertrain syntheses. This process discretizes the cycle into one second lasting quasi-static operational points, which can be seen in **Fig. 7**. These operational points have been interpolated from the e-machine and inverter loss maps respecting:

- Loss-optimal PWM switching frequencies,
- Minimal PWM switching frequencies or
- Constant PWM switching frequencies at 10 kHz.

This finally yields the cycle consumptions in comparison to inverter loss and temperature for these three switching strategies.

5 Results

5.1 System Losses

In **Fig. 8** the evolution over time of the switching frequency for the different operation strategies maximum, minimum, and optimal switching frequency is depicted. In the maximum case, the switching frequency is constant at 10kHz, whereas in the minimum case it is not. This is due to the constraints on the minimal switching frequency, which are a function of the operation state, see Sec. 4.1. In the optimal case, the switching frequency varies mainly between the base points of 1, 4, 7, and 10 kHz. This is also illustrated in the histogram in **Fig. 9**.

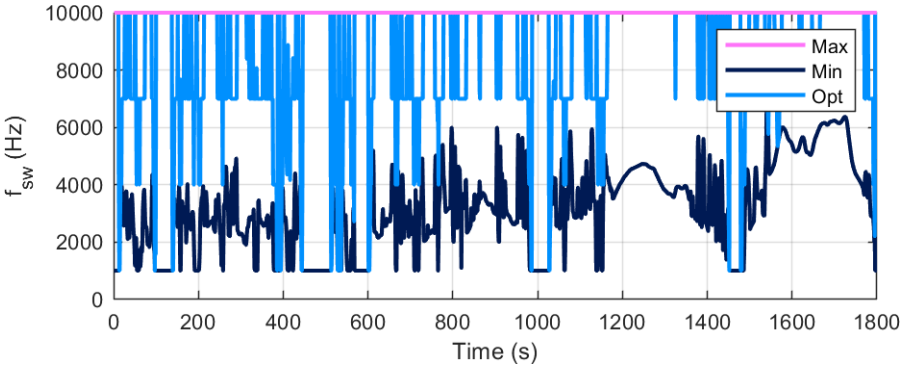

Fig. 8. Switching frequency time series

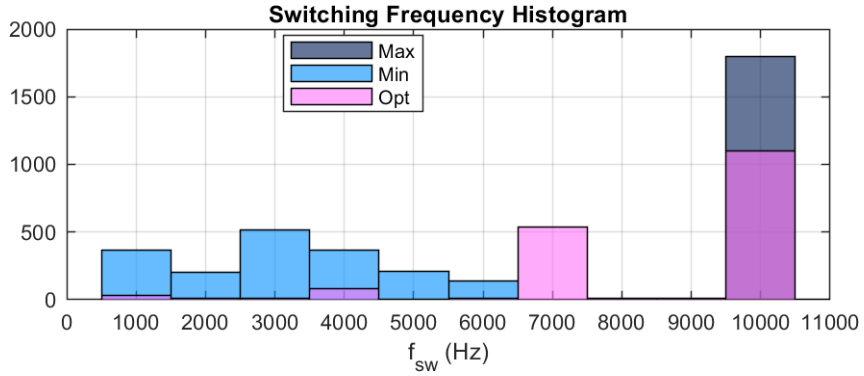

Fig. 9. Switching frequency histogram

The evolution over time of the resulting power losses for the inverter and in combination with the e-machine are illustrated **Fig. 10**. Regarding the inverter losses, using the largest possible switching frequency clearly results in the largest losses and using the minimal switching frequency in the smallest. The optimal case is somewhere in between these two. The losses for the combined system show a different picture. Here, they are largest when the minimal switching frequency is used and minimal if the largest frequency is used. This is because higher switching frequencies cause larger losses in the e-machine and the losses in the e-machine are larger than those in the inverter. Again, the optimal case is somewhere in between the two. This is further detailed in **Table 2**, where we calculate the energy losses over the complete cycle for the different cases. We also compute the relative change w.r.t. the case when the maximum frequency is used throughout the whole cycle. The aforementioned qualitative results are confirmed by the numbers in the table. In addition, we see that in the case of the optimal switching frequency, the overall losses slightly decrease.

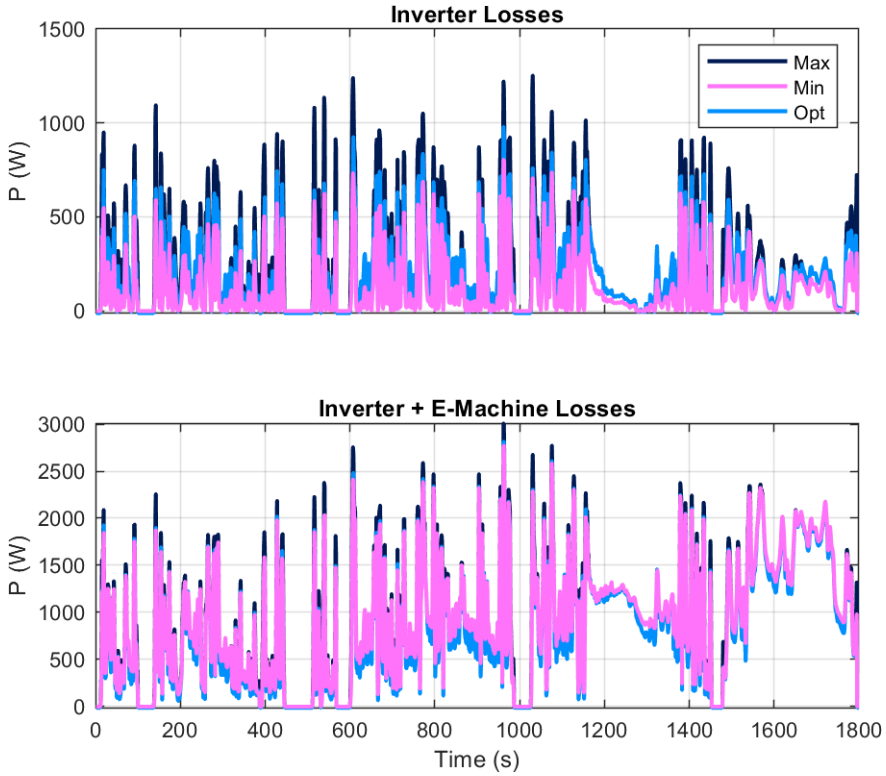

Fig. 10. Time series of power losses

	$f_{sw,max}$	$f_{sw,min}$		$f_{sw,opt}$	
			w.r.t. $f_{sw,max}$		w.r.t. $f_{sw,max}$
Losses e-machine	324 Wh	385 Wh	+18.8 %	331 Wh	+2.2 %
Losses inverter	116 Wh	58 Wh	-50.0 %	92 Wh	-20.7 %
Overall losses	440 Wh	443 Wh	+0.7 %	423 Wh	-3.9 %

Table 2. Comparison of the resulting energy losses

5.2 Lifetime analysis

For the lifetime analysis, the time series of the cycle simulations are fed through a dynamic inverter model (power losses + temperature model) operating in the switching frequency time raster to compute detailed evolutions of the junction temperature and the corresponding temperature swings. The resulting temperature swings are counted

using the Rainflow algorithm and then fed to the LESIT model with parameters for a SiC-MOSFET (**Fig. 11**). The obtained results are given in **Table 3** and show a significant reduction of the lifetime usage for the cases of minimal and optimal switching frequency strategies. This is due to the smaller resulting average temperatures and temperature swings, as shown in **Fig. 12**.

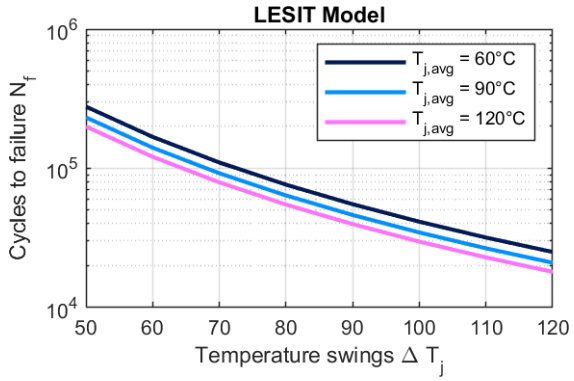

Fig. 11. LESIT model with parameters adapted to [15]

	$f_{sw,max}$	$f_{sw,min}$	$f_{sw,opt}$
Lifetime usage	0.008034 %	0.001429 %	0.003131 %
w.r.t. $f_{sw,max}$		-82.2 %	-61.03 %

Table 3. Results of lifetime analysis with LESIT model

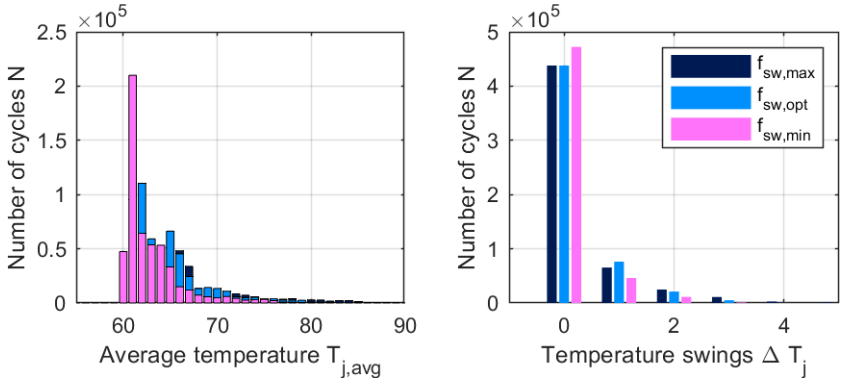

Fig. 12. Rainflow analysis

5.3 **Eddy-current loss**

One important aspect that has been neglected so far is the eddy-current loss in permanent magnets. Even though it hardly impacts the efficiency, it might heavily increase the magnet temperature and with-it demagnetization. One of the most challenging areas of operation is the medium base speed region at high torque (resp. current). In the example of **Fig. 7** this will approx. be found between 2000 rpm and 4000 rpm and shows optimal PWM switching frequencies between 4 kHz and 10 kHz. Here, the voltage modulation index approaches 0.5, which maximizes the current harmonic content and with-it magnet loss. Whereas a switching frequency of 10 kHz leads to max. magnet loss of approx. 200 W in this example, a switching frequency of 4 kHz increases this loss to almost 500 W. Thus, thermal and demagnetization calculations need to account for influences of lower switching frequencies – and might even dictate additional minimal frequencies boundaries in certain areas of operation to protect the e-machine from deterioration.

6 Conclusion

The usage of optimized control strategies leads to an increased lifetime of the power module at (slightly) reduced system losses compared to an operation at nominal frequency. This leads to an increased service life of the inverter. Whether this benefit can be used for a down-sizing of the power module, as suggested in [13], and lead to an immediate cost reduction of the inverter strongly depends on the system specifications and available power modules.

Despite the discussed boundary conditions, the minimal switching frequency is also limited by the NVH behavior and additional magnet loss, which in the worst-case can deteriorate the lifetime of the e-machine. These side-effects and its impact on the e-machine and inverter design are currently under investigation.

The interactions between e-machine, inverter, and operating strategy must be considered during the design phase. The powertrain and component synthesis combine these tasks into one method chain, which allows an optimal reconciliation of the demands for high efficiency, minimal costs, and compactness at a high system reliability for future electric powertrains.

7 Acknowledgements

This work has been performed in the research project “SiC-Mobil – SiC inverters for e-mobility” [14]. This research project is funded by the Federal Ministry of Economic Affairs and Climate Action (BMWK), grant number 19I21024A.

References

1. PGC Consultancy, https://www.pgcconsultancy.com/post/taking-stock-of-sic-part-1-a-review-of-sic-cost-competitiveness-and-a-roadmap-to-lower-costs, last accessed 2023/02/07.
2. PGC Consultancy, https://www.pgcconsultancy.com/post/taking-stock-of-sic-part-2-a-review-of-current-sic-power-devices, last accessed 2023/02/07.
3. Iannuzzo, F., Bahman A. S.: Testing and Modeling of Power Electronic Components for Relibality, In: 23rd European Conference on Power Electronics and Applications EPE ECCE Europe, 2021.
4. Kaminski, N.: From Standard Packages Equipped With SiC Chips Towards True SiC Packages, Tutorial, In: 19th International Conference on Silicon Carbide and Related Materials (ICSCRM) 2022, Davos.
5. Hoffmann, F., Kaminski, N.: Comparison of the Power Cycling Performance of Silicon and Silicon Carbide Power Devices in a Baseplate Less Module Package at Different Temperature Swings, In: 2021 33rd International Symposium on Power Semiconductor Devices and ICs (ISPSD)
6. Yang, Y., Dorn-Gomba, L., Rodriguez, R., Mak, C. and Emadi, A., Automotive Power Module Packaging: Current Status and Future Trends, In IEEE Access, vol. 8, pp. 160126-160144, 2020, doi: 10.1109/ACCESS.2020.3019775.
7. Kaczorowski, D., Michalak, B., Mertens, A., A Novel Thermal Management Algorithm for Improved Lifetime and Overload Capabilities of Traction Converters, In 17th European Conference on Power Electronics and Applications (EPE'15 ECCE-Europe), pp. 1-10, IEEE, 2015.
8. Weckert, M., Roth-Stielow, J., Chances and limits of a thermal control for a three-phase voltage source inverter in traction applications using permanent magnet synchronous or induction machines. In Proceedings of the 2011 14th European conference on power electronics and applications, pp. 1-10, IEEE, 2011.
9. Murdock, D. A., Torres, J. E. R., Connors, J. J., Lorenz, R. D., Active thermal control of power electronic modules. IEEE Transactions on Industry Applications, 42(2), pp. 552-558, 2006.
10. Kuprat, J., van der Broeck, C. H., Andresen, M., Kalker, S., Liserre, M., De Doncker, R. W., Research on active thermal control: Actual status and future trends. IEEE Journal of Emerging and Selected Topics in Power Electronics, 9(6), pp. 6494-6506, 2021.
11. Wintrich, A., Nicolai, U., Tursky, W., Reimann, T., Application manual power semiconductors. SEMIKRON International GmbH, 2015
12. Hoffmann, F., Kaminski, N., Power cycling capability and lifetime estimation of discrete silicon carbide power devices. In Materials Science Forum, Vol. 1004, pp. 977-984, 2020.
13. Kaczorowski, D. and Mertens, A., Reduction of the EV Inverter Chip Size at Constant Reliability by Active Thermal Control, 2016 IEEE Vehicle Power and Propulsion Conference (VPPC), Hangzhou, China, 2016, pp. 1-0, doi: 10.1109/VPPC.2016.7791759.
14. SiC-Mobil Project, https://www.sic-mobil.de/